JOURNAL OF AGRICULTURAL AND FOOD CHEMISTRY

Browning in *Annona cherimola* Fruit: Role of Polyphenol Oxidase and Characterization of a Coding Sequence of the Enzyme

HUMBERTO PRIETO,[†] DANIELLA UTZ,[‡] ÁLVARO CASTRO,[†] CARLOS AGUIRRE,[†] MAURICIO GONZÁLEZ-AGÜERO,[†] HÉCTOR VALDÉS,[§] NICOLAS CIFUENTES,[‡] BRUNO G. DEFILIPPI,[†] PABLO ZAMORA,[‡] GUSTAVO ZÚÑIGA,[‡] AND REINALDO CAMPOS-VARGAS*,[†]

Instituto de Investigaciones Agropecuarias, INIA, Santa Rosa 11610, Santiago, Chile; Facultad de Química y Biología, Universidad de Santiago de Chile, Av. Bernardo O'Higgins 3363, Santiago, Chile; and Facultad de Ciencias, Escuela de Agronomía, Universidad de La Serena, Benavente 980, La Serena, Chile

Cherimoya (*Annona cherimola* Mill.) fruit is an attractive candidate for food processing applications as fresh cut. However, along with its desirable delicate taste, cherimoya shows a marked susceptibility to browning. This condition is mainly attributed to polyphenol oxidase activity (PPO). A general lack of knowledge regarding PPO and its role in the oxidative loss of quality in processed cherimoya fruit requires a better understanding of the mechanisms involved. The work carried out included the cloning of a full-length cDNA, an analysis of its properties in the deduced amino sequence, and linkage of its mRNA levels with enzyme activity in mature and ripe fruits after wounding. The results showed one gene different at the nucleotide level when compared with previously reported genes, but a well-conserved protein, either in functional and in structural terms. Cherimoya PPO gene (*Ac-ppo,* GenBank DQ990911) showed to be present apparently in one copy of the genome, and its transcripts could be significantly detected in leaves and less abundantly in flowers and fruits. Analysis of wounded matured and ripened fruits revealed an inductive behavior for mRNA levels in the flesh of mature cherimoya after 16 h. Although the highest enzymatic activity was observed on rind, a consistent PPO activity was detected on flesh samples. A lack of correlation between PPO mRNA level and PPO activity was observed, especially in flesh tissue. This is probably due to the presence of monophenolic substrates inducing a lag period, enzyme inhibitors and/or diphenolic substrates causing suicide inactivation, and proenzyme or latent isoforms of PPO. To our knowledge this is the first report of a complete PPO sequence in cherimoya. Furthermore, the gene is highly divergent from known nucleotide sequences but shows a well conserved protein in terms of its function, deduced structure, and physiological role.

KEYWORDS: Browning; fresh cut; gene structure; minimally processed; polyphenol oxidase

INTRODUCTION

Cherimoya (*Annona cherimola* Mill.) is an economically valuable fruit of the *Annonaceae* family. It is considered an exotic fruit of warm climates with limited distribution. Cherimoya fruits must be kept at low temperature (i.e., 10 °C) to delay softening during post-harvest. Once the fruit is at room temperature browning occurs very rapidly, particularly after cutting. The high susceptibility to oxidative events makes it difficult to handle the fruit during fresh cut processing and storage. The primary enzyme responsible for fruit browning is polyphenol oxidase (PPO). PPO catalyzes the hydroxylation of monophenols to *o*-diphenols (EC 1.14.18.1) throughout a cresolase/monophenolase activity and a subsequent oxidation of these *o*-diphenols to the corresponding *o*-quinones (EC 1.10.3.1) by a catecholase/diphenolase activity (*1–3*). The formed quinones appear to interact with similar compounds forming black, brown, and red pigments (*4*) that can be interpreted as a stress response of the plant tissues (*5*).

Because of the importance of the browning processes in the food industry, PPO function and its regulation have been studied in several fruits and vegetables (*5–12*). The reaction mechanism for monophenolase and diphenolase activities of PPO has been

* To whom correspondence should be addressed. Phone: 56 2 7575161. Fax: 56 2 7575104. E-mail: rcampos@inia.cl.
[†] Instituto de Investigaciones Agropecuarias, INIA.
[‡] Universidad de Santiago de Chile.
[§] Universidad de La Serena.

10.1021/jf070586+ CCC: $37.00 © 2007 American Chemical Society
Published on Web 10/02/2007

established (*13, 14*). Important and conserved characteristics, according to their proposed reactions, have been established (*15, 16*). Three main regions in the PPO coding sequence (CDS) have been established (*15*): (a) an amino portion with the active site conformed by a dicupric center where each center interacts with three histidine side chains (*17*), (b) a central polylinker area defined by an α-helix rich segment, and (c) the carboxy terminal end, consisting of an extremely rich β-sheet area (*15*).

At the functional level, PPO seems to be confined mainly to plastid compartments (*16, 18, 19*), but variability in protein size and location of active proteins have suggested differences in final targeting (*18, 19*). Transit peptides that post-translationally direct the protein to the chloroplast have been described and analyzed (*16*), and multistep targeting into plastids has been also demonstrated (*18*), although polyphenol oxidase also has been reported in vacuoles (*20*). Additionally, the 5′ flanking regions of many PPO genes have been shown to be highly divergent, leading to speculation that differential gene expression, location, and even functions could take place in species where complex PPO families have been described (*18, 21–23*).

The enzymatic browning of a Spanish cherimoya has been studied by other authors, who have purified a PPO and characterized its monophenolase and diphenolase activities (*24–29*). The browning of an Italian cherimoya has been also analyzed (*30*). As a first attempt for designing fruit processing strategies for fresh cut in an *A. cherimola* variety from Chile, we describe a molecular biology approach focused in the understanding of the role of PPO in the browning process as result of wounding. The cloning of a PPO full-length coding sequence, its characterization through comparative analysis with known data, and a primary functional analysis tying transcript levels and enzyme activities in wounded fruits are described.

MATERIALS AND METHODS

Plant Material. Plants of *A. cherimola* var. "Concha Lisa" were obtained from commercially available sources and kept in the greenhouse until use. New leaves from apical buds were selected and processed for DNA extractions. For specific flower RNA analysis whole flowers (F), leaves (L), and growing (GF) and mature fruits (MF) were harvested and stored at −80 °C until used.

For specific time-course analysis of wounded mature fruits (var. Concha Lisa), fruit samples were harvested from cherimoya trees grown in a commercial orchard located in Quillota, Chile (32°52′S, 71°15′W). Change in fruit color was considered as a harvesting index, a parameter used by the fruit company's technical staff. In general, large- to medium-size fruits were selected and transported to the postharvest laboratory facility at INIA.

PPO Activity and Inhibitor Experiment. PPO activity evaluation was done as in Siriphanic and Kader (*31*) with modifications. Briefly, cherimoya fruit samples were obtained and frozen until preparation. A 4-g sample of cherimoya was ground in 12 mL of buffer [0.1 M citric acid (pH 6.6), 5 mM 2-Me, 0.4 g of polyvinylpolypirrolidone]. The mixture was centrifuged at 20,000*g* for 10 min at 4 °C, and 0.1 mL of supernatant was saved and added to 2.9 mL of buffer [0.5 mM citric acid buffer (pH 6.6) and 20 mM catechol]. The activity was measured in a Shimadzu UV-1700 spectrophotometer as product at 420 nm in 10 min at 25 °C. The straight part of the curve was considered for activity calculations. A blank test containing just buffer or substrate did not show changes in absorbance in the assayed period. The unit for PPO enzyme activity (U) was defined as the change of 0.001 absorbance value under the described conditions. The protein content of enzyme extracts was determined by the method of Bradford (*32*), by using a Bio-Rad protein assay kit and bovine serum albumin (BSA) as a standard. The PPO activity was expressed as U min^{-1} mg^{-1} total protein.

To study the existence of PPO activity inhibitor, 100 or 600 μL of reaction buffer was replace by a similar volume of double distillated (dd) water or flesh crude extract and combine with 100 μL of rind crude extract of cherimoya fruit. The PPO activity was assayed as stated above.

Table 1. Sequences Used for Comparison and Structural Analysis of Cherimoya PPO Gene *Ac-ppo*

specie	common name	accession number
Ananas comosus	pineapple	AF261957
Camellia sinensis	tea	DQ513313
Diospyros kaki	persimmon	AF039165
Ipomoea batatas	sweet potato	AJ309175
Lycopersicon esculentum	tomato	Z12838
Malus domestica	apple	L29450
Medicago sativa	alfalfa	AY283062
Nicotiana tabacum	tobacco	Y12501
Oryza sativa	rice	AL606645
Physcomitrella patens		AY904721
Populus balsamifera subsp. *trichocarpa* x *Populus deltoides*	poplar	AY665682
Populus tremuloides	trembling aspen	AF368291
Prunus armeniaca	apricot	AF020786
Prunus salicina	Japanese plum	AY865623
Pyrus pyrifolia	Japanese pear	AB056680
Solanum tuberosum	potato	U22921
Spinacia oleracea	spinach	U19270
Trifolium pratense	red clover	AY017304
Triticum aestivum	wheat	AY596266
Vicia faba	fava bean	Z11702
Vitis vinifera	grape	Z27411

Sequence Analysis for Primer Design. Public nucleotide and amino acid sequences described for PPO were obtained from the National Center for Biotechnology Information Database (NCBI) (*33*). **Table 1** summarizes analyzed sequences for primer design and sequence, structural, and functional analysis. Available genes were translated into deduced amino acid sequences using the "Translation" tool from the OMIGA 2.0 package (Oxford Molecular Ltd., U.S.). Obtained sequences were then aligned using Clustal W analysis from the BioEdit 7.0.5.2. package (*34*). Conserved regions, essentially belonging to the active site of PPOs and its surrounding areas, were evaluated as putative target areas for PCR amplification. Visual evaluation on conserved regions and further software analysis were carried out to design degenerate and universal primer sets. PPO universal set primers were developed by the "Universal" protocol from PrimerMaster 1.0 (Vitali Proutski, St. Petersburg, Russia). Primers were synthesized by Integrated DNA Technologies (Coralville, U.S.).

RNA Extraction. Total RNA from *A. cherimola* tissue was extracted following the protocol described by Chang et al. (*35*). Briefly, 4–5 g of frozen tissue was ground using liquid nitrogen in a mortar and then transferred into a 50-mL Falcon tube with preheated (65 °C) extraction buffer (CTAB 2%, PVP 2%, Tris-HCl 100 mM pH 8.0, EDTA 25 mM, NaCl 2.0 M, 0.5 g spermidine, 2-mercaptoethanol 2%) and incubated 20 min at 65 °C. The mixture was cleared by two extractions with an equal volume of chloroform/isoamyl alcohol (24:1). To separate the phases, phenolic extractions were centrifuged at 12,000*g* for 30 min at 4 °C, and the aqueous phase was precipitated applying 0.25 of total volume of LiCl 10 M. The product from the precipitation reaction was kept overnight at 4 °C and then collected by centrifugation at 12,000*g* for 20 min at 4 °C. The pellet was dissolved with 500 μL of preheated (65 °C) SSTE buffer (NaCl 1.0 M, SDS 0.5%, Tris-HCl 10 mM pH 8.0, EDTA 1.0 mM) and transferred into a fresh 1.5-mL tube. A new phenolic extraction was applied using 500 μL of chloroform/isoamyl alcohol (24:1), and phases were separated by centrifugation at 14,000*g* for 15 min at room temperature. The aqueous phase was precipitated by adding 2 volumes of ethanol 100% and incubated at −80 °C for 30 min. The pellet was obtained by centrifugation at 12,000*g* for 30 min at 4 °C. The supernatant was discarded, and the pellet was washed with 75% cold ethanol and then allowed to dry at 50 °C. The final pellet was resuspended with 50 μL of DEPC-treated sterile water.

DNA Extraction. Genomic DNA was extracted from young leaves of *A. cherimola* trees, following the procedures of Steenkamp et al. (*36*). A 0.1-g sample of tissue was mixed with 750 μL of extraction buffer

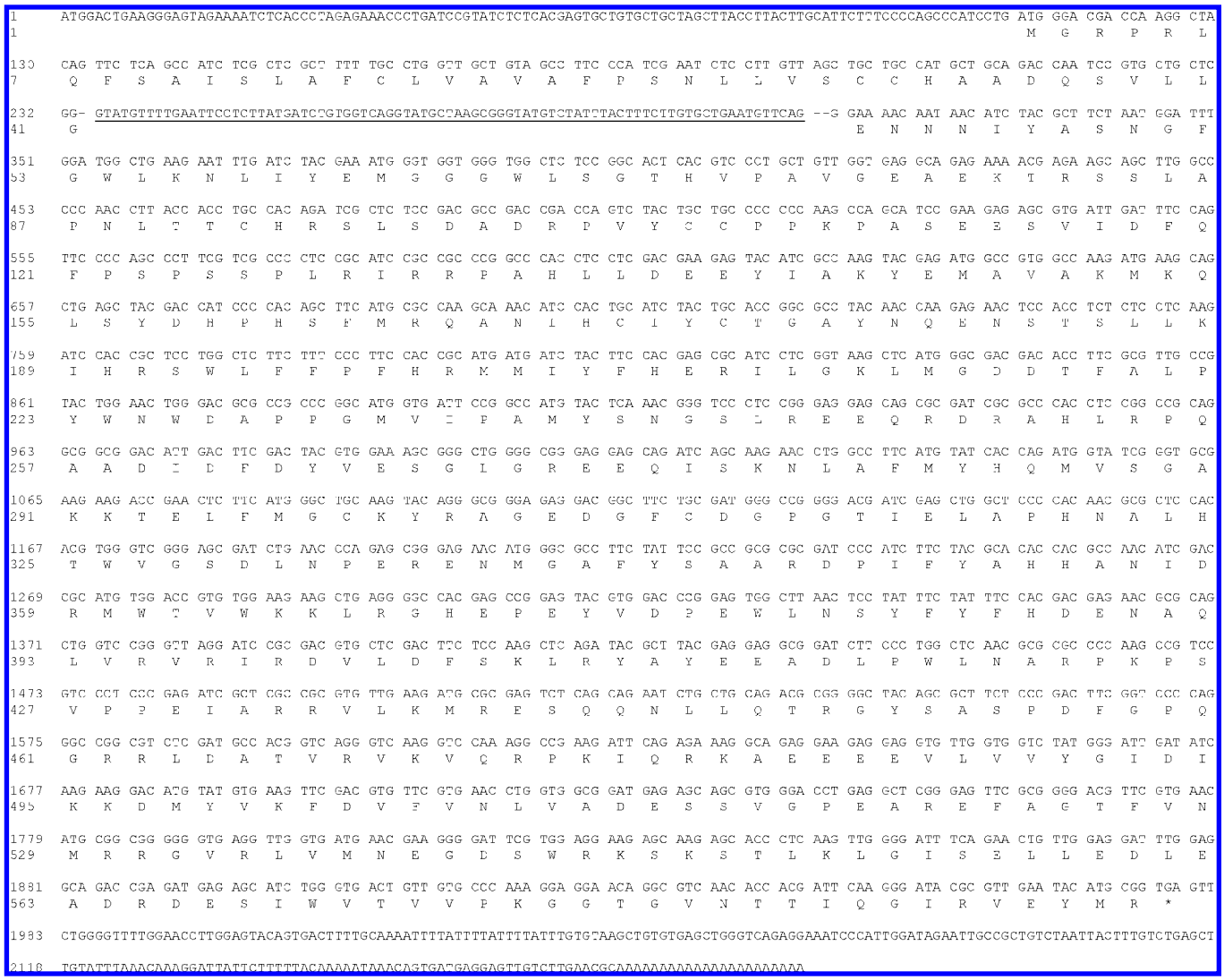

Figure 1. Complete coding sequence of *A. cherimola* polyphenol oxidase and its 5′- 3′ - UTR regions. Nucleotide (*Ac-ppo*) and deduced amino acid (Ac-PPO) sequences of a fruit polyphenol oxidase from *A. cherimola* is shown. 5′ and 3′ RACE on cDNA templates were also determined and sequence of nucleotides after and before CDS is shown. Intron sequence at 5′ end of the CDS, between nucleotides 234 and 317, is indicated (underline).

(CTAB 3% w/v; Tris-HCl 1 M pH 8; NaCl 1.4 M; EDTA 20 mM), 15 μL of 2-mercaptoethanol, and 0.1 mg of PVP. The tissue grinding was done with a Minibead Miller (Biospec Products, Batlesville, OK) for 3 min and then incubated at 65 °C. Next, 750 μL of chloroform/isoamyl alcohol (24:1) was added to the mixture, which was centrifuged at 10,000*g* for 10 min at 4 °C. The aqueous phase was precipitated adding 0.66 of isopropanol and incubating at −20 °C overnight. The pellets were obtained by centrifugation at 10,000*g* for 10 min at 4 °C and then washed with 1 mL of 76% cold ethanol for 30 min. Pellets were centrifuged as before, allowed to dry, and resuspended in 1 mL of ddH_2O. Two microliters of RNase A (1 mg mL^{-1}) was added to the DNA extractions, and the tubes were incubated for 30 min at 37 °C.

Cloning of Full Length *A. cherimola* PPO (AcPPO) cDNA. To obtain a full-length cDNA, total RNA was extracted from immature fruits (4 cm diameter) and retro-transcribed into cDNA using technical components and procedures from a GeneRacer kit (Invitrogen). cDNAs were then evaluated as template source for PCR amplifications using different combinations of previously designed primers (*37*, *38*) and newly synthesized. From all evaluated possibilities, the combination of three new degenerate oligos, AcPPO-a2 (reverse, 5′ TIC KRT CIA CRT TNG CRT GRT G 3′); AcPPO-s2 (forward, 5′ GGY TIT TYY TYC CIT TYC AYM G 3′); and AcPPO-s3 (forward, 5′ GGY TIT TYY TYC CIT TYC AYM G 3′), successfully generated reproducible and consistent fragments. These fragments were cloned by using pGEMT-Easy (Promega) system, and the clones were sequenced automatically at Macrogen (Chongro-ku, Seoul, Korea). The obtained information was used as anchor sequence for designing specific AcPPO oligos and 3′ RACE and 5′ RACE amplifications. Primers used for 3′ RACE and 5′ RACE, respectively were AcPPO-1050 (forward, 5′ ACT CAA ACG GGT CCC T 3′) and AcPPO-Rev (reverse, 5′ CGA TCC CAT CTT CTA CGC ACA 3′). RACE amplifications were carried out using the adaptors, primers, enzymes, and procedures from the GeneRacer kit. Amplified 3′ and 5′ RACE fragments were analyzed by agarose gel electrophoresis, and selected bands were purified using the QIAquick gel extraction kit (QIAgene). DNA fragments were cloned into Topo PCR4 vectors (Invitrogen) according to manufacturer's recommendations, and both strands were sequenced. Keys for degenerated bases are R = A,G; Y = C,T; M = A,C; K = G,T; N = A,C,G,T.

Sequence Analysis of *A. cherimola* PPO Coding Sequence (CDS). The obtained PPO sequence from cDNAs isolated from *A. cherimola* fruits was compared primarily using the BLASTn tool (*39*) from NCBI. Similarities analyses were performed using ClustalW in the BioEdit 7.0.5.2 package. Deduced amino acid sequence was obtained and compared using the BLASTx tool (*39*) from the same site. Basic signals to deduce the best CDS in the candidate sequence were carried out using GeneScan (*40*) Full CDS translation was carried out by using the "Translate" tool from the Omiga 2.0 package. Lineal processing of deduced sequences and comparison with previously reported and deduced sequences were carried out using Neighbor-Joining (*41*) linked to Kimura's two parameters (*42*) throughout BioEdit 7.0.5.2. N-Terminal sequence analysis was carried out by using iPSORT (*43*) and Signal IP 3.0 (*44*). Secondary structure analyses were carried out using Jpred

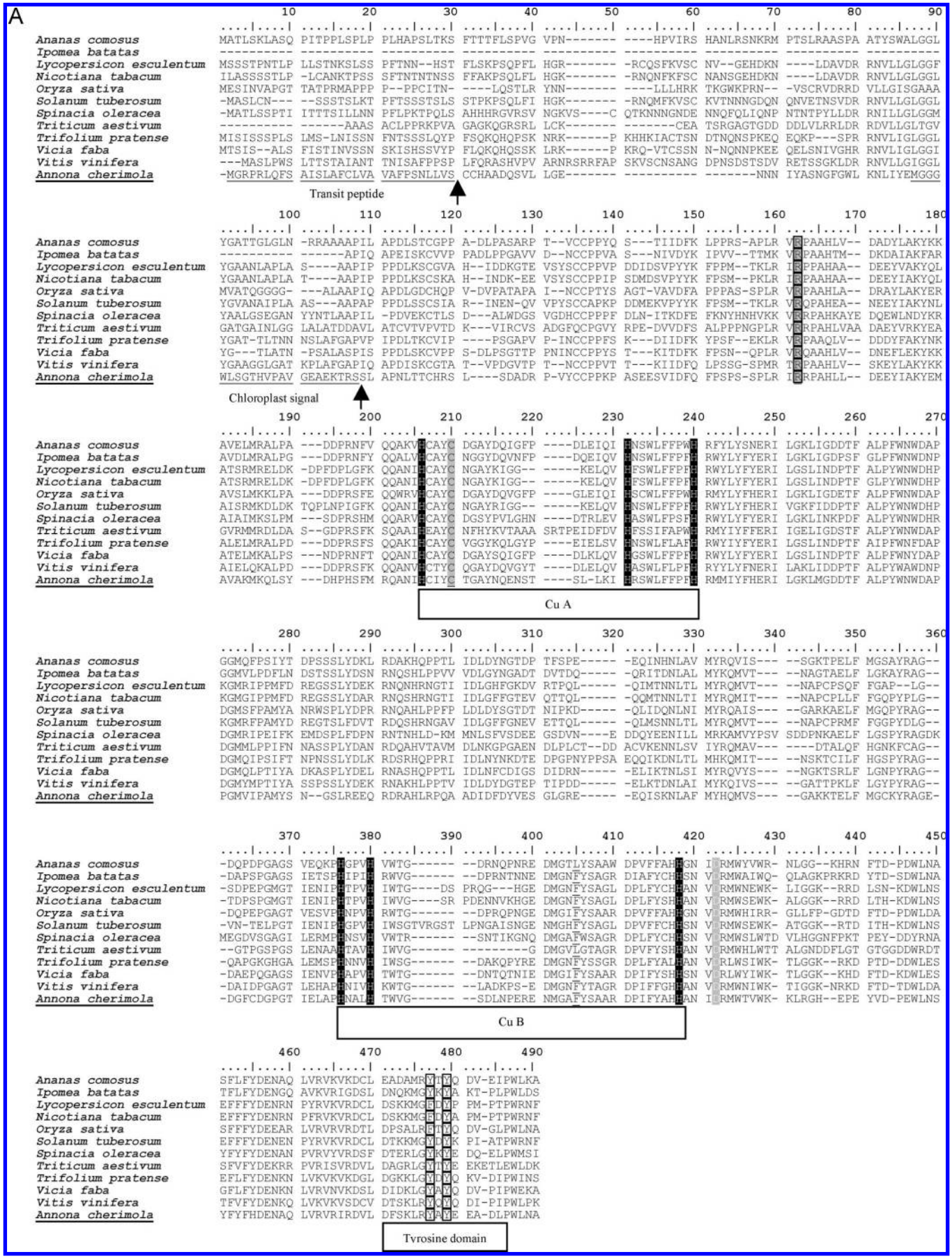
A
Ananas comosus
Ipomea batatas
Lycopersicon esculentum
Nicotiana tabacum
Oryza sativa
Solanum tuberosum
Spinacia oleracea
Triticum aestivum
Trifolium pratense
Vicia faba
Vitis vinifera
Annona cherimola
Transit peptide
Chloroplast signal
Cu A
Cu B
Tyrosine domain

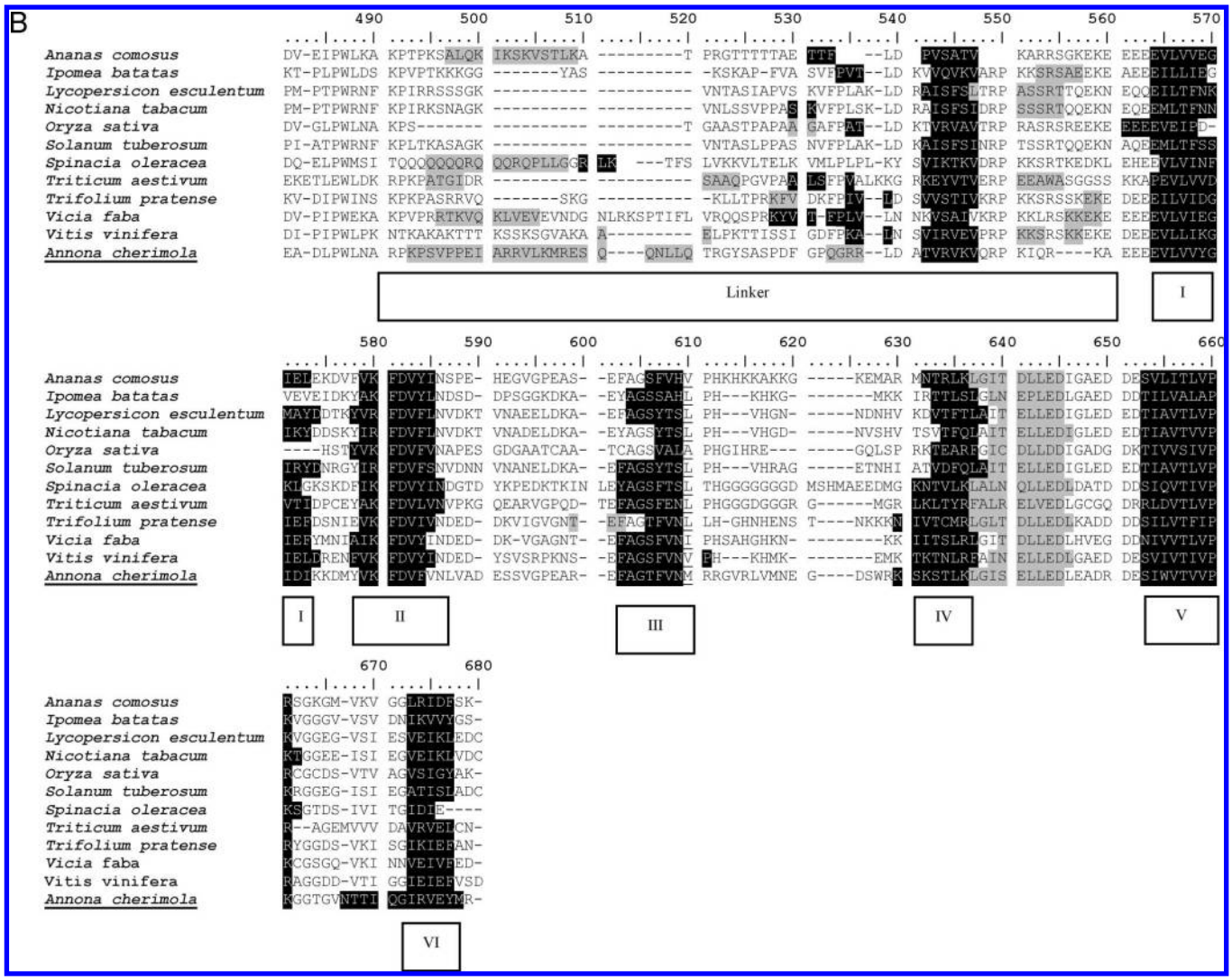

Figure 2. Functional and structural comparison of deduced *A. cherimola* PPO. Based on a pipeline proposed by Marusek et al. (*15*), bioinformatic tools were selected to analyze the N- (**A**) and C- (**B**) terminal segments of currently described and *A. cherimola* PPOs. (**A**) N-Terminal analysis with the two active sites (copper A and B) shown (squares CuA and CuB), including their conserved histidines (white H in black box); cysteine of the proposed structural thioether bridge (black C in gray box) and a tyrosine motif (square) with a couple of residues (black Y in white box) marking domain termini. Arginine (black R in gray box) and aspartic (white D in gray box) residues that interact with the Y motif, throughout of π-cation and hydrogen bond, respectively, were also detected. Gate residues (F or L) inside of copper B active site are also found. Transit peptides have been also included in this comparison, showing the proposed signal (underlined) for the *A. cherimola* PPO and its putative cleavage site (arrow). In all of the included sequences, processed proteins are postulated to start at residue 107, which is still undefined in case of an *A. cherimola* unripe protein. (**B**) C-Terminal region analysis, showing the proposed linker area (linker), rich in α-helix structure (black n in gray box), followed by six strands of β-sheet structure (white n in black box) (squares I–VI), in which an inserted α-helix could be found between strands IV and V. The active site regulator residue, ending strand III, is also shown (n).

predictor (*45*) on deduced proteins previously aligned by BLASTx. Specific PPO secondary structure analysis was also carried out using the PSIPRED method (*46*) on PSIPRED Server (*47, 48*).

Southern Blot. A 20-μg sample of genomic DNA was digested with *Eco*RI and *Hind* III enzymes (New England Biolabs, Ipswich, MA), separated on 0.8% agarose gel, and then transferred to nylon Hybond N+ membranes (Amersham). Hybridization was performed following procedures indicated by the manufacturer, hybridizing at 60 °C with a ^{32}P-labelled probe in the presence of hybridization buffer (5x SSPE, 5x Denhardt's, 100 μg of sheared DNA, 0.5% w/v SDS, formamide 30%). The membrane was washed at room temperature for 5 min with Solution I (2x SSC, 0.1% w/v SDS) and then at 68 °C for 15 min with Solution II (0.2x SSC, 0.1% w/v SDS). Detection was carried out using the Personal Molecular Imager FX (BioRad) using Quantity One 4.4.0 software.

Northern Blot. A 20-μg sample of total RNA from samples taken from different tissues and fruit samples obtained at different times post-wounding were separated on a 1.2% denaturating agarose gel containing 10% formaldehyde. The RNA was transferred to nylon Hybond N+ membranes (Amersham). Hybridization was performed following the procedures indicated by the manufacturer. Briefly, the blots were hybridized at 60 °C with a ^{32}P-labelled probe in presence of hybridization buffer (0.5 M sodium phosphate (pH 7.1), 2 mM EDTA, 7% (w/v) SDS, 0.1% sodium pyrophosphate, formamide 35%). Membranes were washed at room temperature for 5 min with Solution I (1x SSPE, 0.5% w/v SDS) and then at 60 °C for 15 min with Solution II (0.2x SSPE, 0.1% w/v SDS). Detection was carried through Personal Molecular Imager FX (BioRad) using Quantity One 4.4.0 software.

PPO mRNA Quantification by Real-Time Quantitative PCR Assays (qPCR). Quantitative PCR was performed with the real-time PCR system LightCycler (Roche Diagnostics, Mannheim, Germany), using SYBR Green as fluorescent dye to measure DNA amplification products derived from the RNA. A 2-μg sample of RNA was used as template for reverse transcription reactions to synthesize single strand cDNA, using MMVL-RT reverse transcriptase (Promega, Madison, WI) and oligo dT primer (Invitrogen, Breda, The Netherlands), according

to standard procedures. Gene-specific primers were designed by using Primer Premier 5.0 software (Premier Biosoft International, Palo Alto, CA) and synthesized by IDT (Coralville, San Diego, CA). The primers forward and reverse used for amplification of each gene were, respectively, AcPPO-F (5′-ACTCAAACGGGTCCCT-3′) and AcPPO-R (5′-CGATCCCATCTTCTACGCACA-3′); Ac18S rib-F (5′-CCTGAGAAACGGCTACCACATC-3′) and Ac18S rib-R (5′-CATCCCAAGGTCCAACTACGAG-3′). For each gene a calibration curve was performed by measuring the fluorescence of four serial dilutions (10^1 to 10^{-2} pg μL^{-1}) of a plasmid bearing the fragment to amplify that served for the estimation of copy number in total cDNA.

The amplification reaction was carried out in a total volume of 20 μL containing 1 pmol of each primer, 5 mM $MgCl_2$, 1 mL LightCycler DNA Master SYBR Green I (containing 1.25 units of *Taq* polymerase, 10X *Taq* buffer (500 mM KCl, 100 mM Tris- HCl, pH 8.3), dNTPs each at 2 mM, 10X SYBR Green I; Roche Diagnostics) and 100 ng of cDNA prepared as described above. The amplification protocol comprised four phases: (i) denaturation of the template DNA, (ii) amplification of the target DNA, (iii) melting curve analysis for product identification, and (iv) cooling the rotor and the thermal chamber. The initial template denaturation and "hot start" was at 95 °C for 10 min, followed by 35 three-step cycles of template denaturation at 95 °C with a 2 s hold, primer annealing at 60–65 °C for 15 s, and extension at 72 °C for 25 s. Fluorescence data were collected after each extension step. Melting curve analysis was performed by heating the template at 95 °C with a 0 s hold, then cooling to 65 °C with a 15 s hold, and finally raising to 95 °C with a 0.1 °C s^{-1} temperature transition rate while continuously monitoring the fluorescence. All other phases were performed with a 20 °C s^{-1} transition rate. Fluorescence was analyzed using LightCycler analysis software. The crossing point for each reaction was determined using the Second Derivative Maximum algorithm and manual baseline adjustment. The melting curves were checked for single peaks, and the product size of amplifications was confirmed in an agarose gel to ensure the absence of nonspecific PCR products. Triplicate quantitative PCR experiments were performed for each sample, and the expression values were normalized against *18S ribosomal* gene (indicated as Expression in arbitrary units (AU), **Figures 3** and **5**). To test whether *18S ribosomal* behaves as a housekeeping gene in the analyzed samples, cDNA samples from the entire set of samples analyzed by qPCR were synthesized from total RNA with *dap* spike mRNA [*Bacillus subtilis* dehydrodipicolinate reductase, (*49*)] added as internal control (0.01%). For each cDNA, transcript abundances *18S ribosomal* and *dap* were determined by qPCR, and the ratios of control transcript to the endogenous transcript *18S ribosomal* were calculated. The results indicated that the abundance of *18S ribosomal* mRNA remains stable between samples (data not shown).

Statistical Analyses. For PPO activity and qPCR assays there were at least three replicates for evaluation. Data were subjected to analyses of variance and means were separated by LSD test at the 5% level of significance using Statgraphics Plus 5 (Manugistics, Inc., Rockville, MD).

RESULTS

Cloning and Characterization of a Deduced PPO from Fruit. Previously published degenerate primers did not successfully generate the expected PPO-related sequence upon nucleotide (BLASTn) or deduced amino acid (BLASTx) analyses, using either DNA or cDNA as templates. From the newly developed oligos, two couples defined by the reverse AcPPO-a2 and forward AcPPO-s2 and AcPPO-s3 primers generated consistent and reproducible bands of 500 and 700 pbs (respectively) on cDNAs from immature fruit and leaves. The deduced peptides of these fragments showed characteristics corresponding to N-terminal regions of PPOs (*15*), i.e., complete CuB and incomplete CuA centers of the enzyme. Use of specific primers deduced from these segments in 5′ and 3′ RACE generated additional sequences that allowed the assembly of a putative full length cDNA of 2121 base pairs (bps) (**Figure 1**) for a PPO of *A. cherimola* (*Ac-ppo*). Subsequently, the size of 2.1 Kb of *Ac-ppo* was confirmed by Northern blot analysis (data not shown). An exhaustive study of this candidate sequence revealed a CDS consisting of 1785 bps (**Figure 1**), with very low similarity at nucleotide level (as demonstrated by BLASTn) with previously reported sequences but with a high conservation in functional and structural motifs when deduced amino acid sequence was compared with protein databases throughout BLASTx.

Deduced protein (Ac-PPO) is 595 amino acids, with theoretical pI/Mw: 6.43 / 67,811.18 and a putative transit peptide of approximately 29 residues, which is predicted to be processed at the LLVS/CR motif (**Figure 2A**). From the remaining peptide, a second targeting signal which sorts the protein into chloroplasts is located on the next 54 amino acids, generating a putative cleavage site in the KTRS/SL motif in the CDS. Structural analysis on the N-terminal end, showed that, in spite of its high difference at nucleotide level, deduced Ac-PPO is conserved in all the key motifs and residues for a typical PPO (*15, 16*) (**Figure 2A**). Two active sites defined as CuA and CuB centers were found in the protein, as expected for a type 3 tyrosinase in which each center has 3 H residues (*17*); a conserved C (C, **Figure 2A**) that has been described to play a structural role interacting throughout a thioether bridge with those H residues in CuA (*50*); a gate residue (F), inside of CuB, proposed as function regulator (*17*); a "tyrosine motif" downstream CuB, with two Ts which should sterically interact through hydrogen bonds with a D, located four residues away from third H in CuB *(15, 51).* Additional stability residues were also found in AC-PPO, as an R residue heading the N-terminal, which should interact with the first T residue in the tyrosine motif; such interaction should generate a stabilized zone by electron π-cation interactions (*15*). In the central segment (or linker region in **Figure 2B**), an α-helix rich zone was found, as previously described for all out of the PPO sequences analyzed (*15*). Additionally, in the C-terminal domain, six β-sheet strings were distinguished (I to VI), with an α-helix between strings IV and V. Additionally, in the Ac-PPO the proposed less-bulky residue assigned as a "regulator" for the active site in PPOs is replaced by M instead of L, as in most of enzymes (*36*) (**Figure 2B**).

To have a better understanding regarding the arrangement of *Ac-ppo* in the *A. cherimola* genome, a Southern blot analysis was made. Nucleic acids hybridization was performed on digested genomic DNA preparations using a conserved segment of the proposed gene (nucleotides 636–1045 in **Figure 1**). The results showed a pattern of one consistent band, suggesting that at least one PPO gene can be found in the genome of *A. cherimola* (data not shown). In parallel, use of *A. cherimola* genomic DNA as template in PCRs carried out with flanking primers designed from 5′- and 3′-border sequences in the CDS not only generated the corresponding genomic copy of the gene but also revealed the existence of a short intron, 83 bps in length, located at the 5′ end of *Ac-ppo* (**Figure 1**).

PPO Gene Expression in Cherimoya and Enzymatic Oxidative Events. PPO mRNA transcript quantification in different cherimoya organs was studied (**Figure 3**). The results show that PPO transcript is present in all tissues sampled. However, PPO mRNA in leaves was significantly higher than in the other organs assayed, followed by flower and fruit tissue.

As an attempt to understand the role of PPO in the browning process of mature and ripe wounded fruits, measurements of enzyme activities and *Ac-ppo* mRNA levels were carried out. Pattern of activities recorded for wounded rind (exocarp) showed higher PPO activity than in flesh (mesocarp) in mature and ripe cherimoya fruits (**Figure 4A** and **B**), although exocarp and mesocarp activities showed a steady level after wounding. The abundance of PPO mRNA of mature and ripe cherimoya rind and flesh tissues after wounding as result of processing were

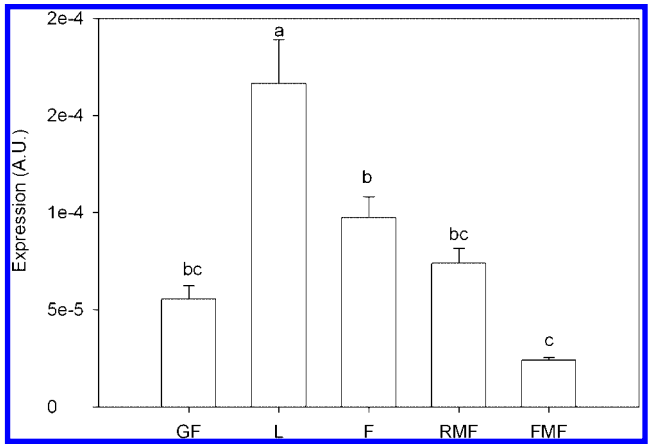

Figure 3. PPO mRNA quantification by qPCR in different cherimoya organs. Basal PPO mRNA levels is observed in growing (GF) and unripe fruits rind (RMF) or flesh (FMF) and higher level of expression was obtained in leaves (L) followed by flowers (F). Triplicate quantitative PCR experiments were performed for each sample, and the expression values were normalized against *18S ribosomal* gene indicated as expression in arbitrary units (AU). Bars atop SE. Bars followed by different small letter are significantly different at $p \leq 0.05$.

studied (**Figure 5A** and **B**, respectively). In mature cherimoya fruit, the pattern of PPO mRNA accumulation in rind did not show statistical differences after processing. However, in the case of flesh samples, after 16 h it was possible to detect a significant accumulation of PPO transcript as a response of wounding. In ripe cherimoya fruit samples, neither rind nor flesh samples showed statistical difference after wounding.

Considering that the PPO activity in the rind was significantly higher than the in flesh and the pattern of PPO mRNA accumulation in the flesh did not show an increment of PPO activity, an experiment to address the possibility to detect inhibitors of PPO activity was made. The activity of the flesh of mature cherimoya was not affected when 100 μL of water was added to the reaction mixture as compared with the original reaction buffer (**Table 2**). However, when 100 μL of crude extract of flesh was added to the reaction mixture, the PPO activity was significantly reduced. This was confirmed when 600 μL of crude extract of flesh was added to the reaction mixture reducing almost totally the PPO activity. The latter was not the case when 600 μL of water was assayed together with rind crude extract. Similar results were obtained when rind crude extract of ripe cherimoya was assayed mixed with flesh crude extracts (data not shown).

DISCUSSION

From degenerative primers designed against known PPO, a candidate *Ac-ppo* gene has been cloned and sequenced. The comparison of *Ac-ppo* with other published genes demonstrated it is highly divergence in terms of nucleotide sequence. This situation could explain the lack of amplification of a consistent band when published degenerated primers were evaluated. It is interesting that the presence of an intron (83 bps) found in the genomic cherimoya PPO sequence has been described in other described PPO genes, such as banana (85 bps (*37*)), wheat (191 and 125 bps (*52*)), and moss (94 bps (*53*)).

Despite the low similarity at the DNA level, the comparison of the deduced amino acid sequence for this gene (Ac-PPO) with other PPOs (which have been structurally processed by Marusek et al. (*15*); **Table 1**) by Neighbor-Joining coupled to Kimura's two parameters (*41, 42*) established a nonrooted tree positioning the Ac-PPO in a cluster constituted by PPOs from species as *I. batatas*, *L. esculentum*, *N. tabacum*, *S. tuberosum*, *S. oleracea*, and *T. aestivum*, which was separated away from sequences described for *O. sativa* and *A. comosus* PPOs (data not shown).

Our analyses showed that Ac-PPO keeps remarkable properties corresponding to a type 3 copper protein (*17*). Conserved motifs are kept not only in the proposed active centers, but considering also basic and strategic amino acids related to active site accessibility, protein structure and stability. Moreover, when already considered key amino acids were not conserved in the Ac-PPO, a structural-functionally compatible residue was found (for instance the active site regulator, as proposed Cuff et al. (*50*)). Amino terminal signals that finally direct Ac-PPO into chloroplasts and putative cleavage sites were also found (**Figure 2**); however, additional experimental data (currently under development) is required to demonstrate this proposed sorting and putative processing of Ac-PPO protein.

The abundance of PPO mRNA was quantified by qPCR, indicating that leaves showed a significantly higher amount of PPO transcript, followed by flowers and fruit tissue (**Figure 3**). The presence of PPO mRNA in all assayed tissues could be explained by a PPO role in defense and disease resistance (*54, 55*). It is possible that the high expression of PPO in leaves is due to the condition of perennial organs in cherimoya trees (*56*) in consequent, leaves remain active for long time being exposed to pathogen or herbivore attack.

The role of this proposed *Ac-ppo* and its putative gene product was contextualized within the browning process, which is observed as soon as ripe fruits are processed, mimicking fresh cut. Measurements of PPO activities on rind samples (**Figure 4A** and **B**) suggested a masked role of the specific gene product, because high levels of enzyme activity were obtained along the whole experiment, whereas mRNA levels of the gene were not significantly induced in rind after wounding in ripe or unripe cherimoya fruit (**Figure 5A** and **B**). In flesh, no inductive pattern can be deduced from PPO activity (**Figure 4A** and **B**), which did not correlate with the significant increase of PPO transcript after 16 h wounding in flesh of unripe fruit (**Figure 5A**), higher than those observed in rind or flesh of ripe cherimoya (**Figure 5B**). From those results, an apparent role of background levels of the enzyme in the general oxidation events registered after wounding can be deduced. We tried to explain the difference between rind and flesh cherimoya PPO activity, since these were evident either in unripe and ripe cherimoya tissue assayed.

The possibility of the existence of an inhibitory agent should be considered taking into account the data showed in **Table 2**, where the PPO activity of rind samples was reduced proportionally to the amount of flesh crude extract added to the reaction mixture. Therefore the results demonstrated the presence of some compound(s) in the cherimoya flesh tissue that can interfere in the PPO activity of the flesh explaining in some way the differences between rind and flesh activity and the lack of increase of flesh PPO activity after 16 h wounding despite of high PPO mRNA. The nature of this or these compound(s) is unknown at this moment.

However, several endogenous, natural enzyme inhibitors are already under discussion (*5, 57*). One possibility is the presence of monopenolic substrates of PPO that induce a lag period prior to the attainment of the steady state rate (*58, 59*). On the other hand, marked levels of PPO activities, determined by PAGE coupled to an in situ assay, have been described for tomato, radish, and oriental melon extracts that previously did not showed detectable enzyme activities (*57*). Sullivan et al. (*60*) described that the PPO activity of crude extract of red clover

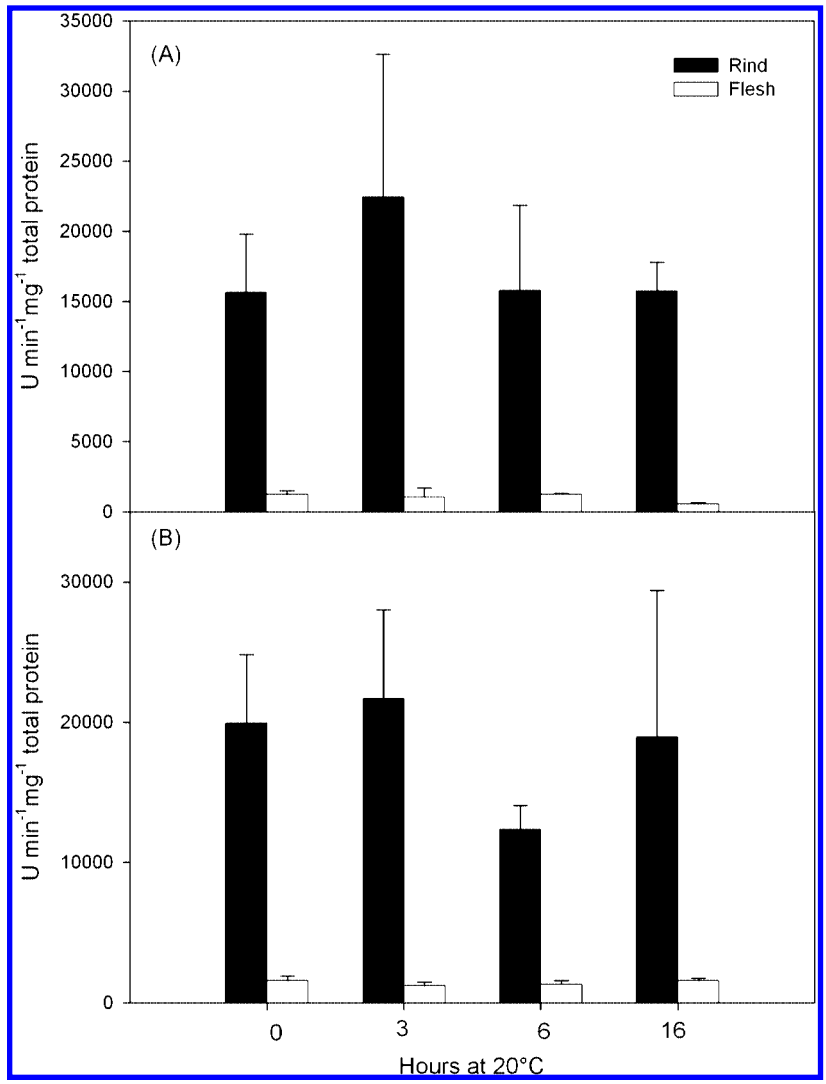

Figure 4. PPO activity determined in unripe (**A**) and ripe (**B**) fruits after wounding on time course analysis at 20 °C (0 to 16 h). Whole unripe and ripe fruits were wounded and then split into rind and flesh tissues, and enzymatic activity was measured. Bars atop SE.

was rapidly inhibited by compounds of low relative molecular mass. Martínez-Cayuela et al. (*61*) studying partially purify cherimoya PPO found that phenolics compounds associated to carboxylic group and benzene nucleus can inhibit the activity of PPO. Some endogenous reductants can remove the quinones generated by PPO, which makes the detection of its enzymatic activity difficult (*28*). Furthermore, diphenolic substrates of PPO can originate the suicide inactivation of the enzyme (*62, 63*). The presence of monophenols, inhibitors, and suicide substrates could be greater in the hydrated flesh than in the lignified rind.

However, it is possible that cherimoya PPO protein shares the same protein processing postulated for PPO protein in grapes (*64*), where unripe PPO requires being processed to be active. An additive mechanism, in which the de novo synthesis of PPO acts sinergically with a preformed enzyme as a general response to wounding, has also been observed in several species such as banana (*37*), potato (*13*), and apricot (*16*). Therefore the results of qPCR could show us the amount of immature cherimoya PPO, and we lack the information of mature active protein that correlates with the PPO activity. In order to answer this question the possibility of raising PPO cherimoya antibody remains to be explored. The presence of proenzyme and/or latent isoforms should be considered in further studies (*65, 66*), which could be particularly relevant considering that the proposed AcPPO gene was detected in a single copy (deduced by Southern blot analysis, not shown), and we did not detect any different sequence by additional experimental approaches focused on 5′- and 3′-ends at UTR regions of the PPO gene.

The difference in level of PPO expression and activity has been described in other species. Sullivan et al. (*60*) mentioned that red clover PPO activity remains high despite a low PPO transcript level, speculating that red clover PPO protein must be stable. A similar conclusion was stated by Chevalier et al. (*9*) in apricot and Gooding et al. (*37*) in banana. Also, we can not exclude supplemental technical artifacts. Although we have used one of the most common quantitative assays for extracted PPO, determining the rate of *o*-quinone formation from catechol by spectrophotometrically assaying the increase in absorbance at 420 nm (*67–77*), properties of PPO from different sources including K_m, optimum pH, and temperature have been extensively studied, and some important differences among K_m values and even optimal pH values have been observed from those analysis. On this basis, an additional explanation for the absence of the concrete relationship between mRNA levels and enzyme activities using this experimental approach can be derived from the assumption that catechol is not a right substrate for this specific cherimoya PPO. This idea could be reinforced by further HPLC experiments on fruit extracts, which have shown diminished in vivo levels of some expected specific PPO substrates, such as naringenin and kaempherol, (*20, 78*) at the

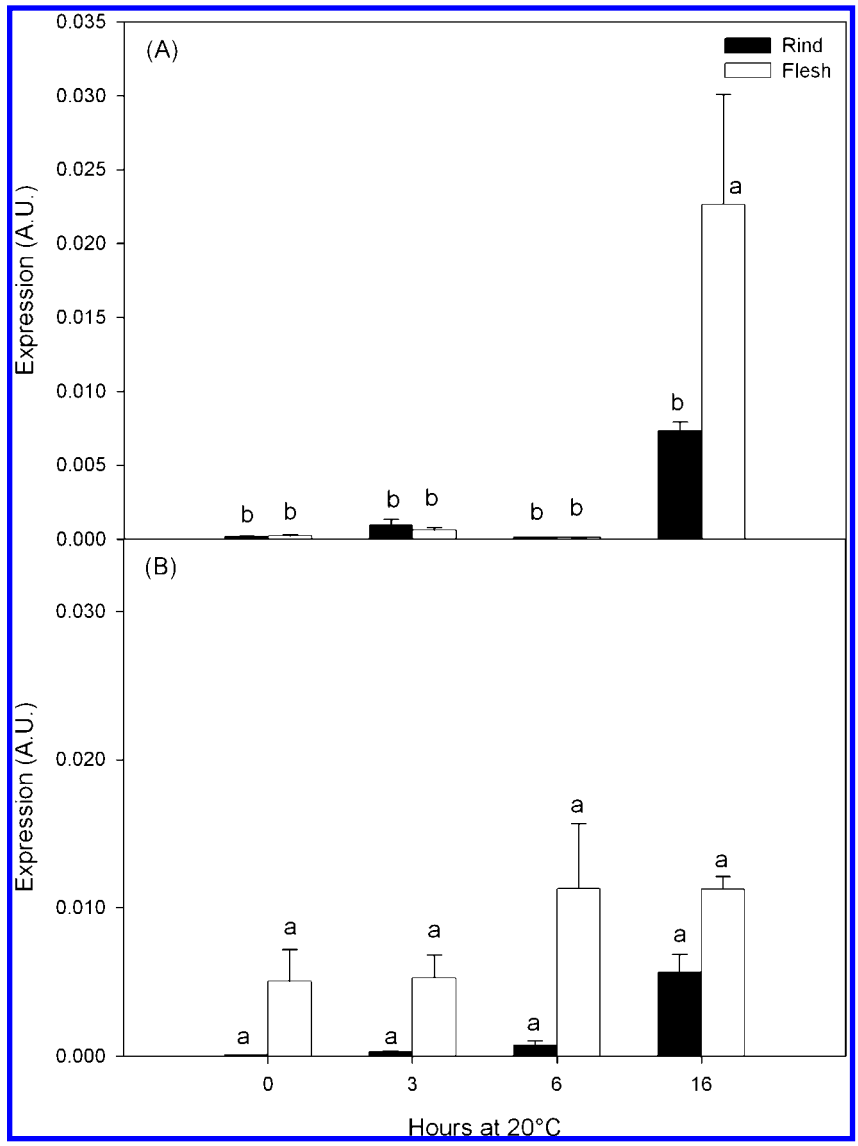

Figure 5. PPO mRNA quantification by qPCR on time course analysis at 20 °C (0 to 16 h) after wounding in unripe (**A**) and ripe (**B**) fruits in rind (exocarp) and flesh (mesocarp). Triplicate quantitative PCR experiments were performed for each sample, and the expression values were normalized against *18S ribosomal* gene indicated as expression in arbitrary units (AU). Bars atop SE. Bars followed by different small letter are significantly different at $p \leq 0.05$.

Table 2. PPO Activity of Unripe Cherimoya Rind Crude Extract and Its Changes as Function of Addition of Flesh Crude Extract in the Reaction Mixture

reaction mixture	PPO activity (U min^{-1} mg^{-1} total protein)
reaction buffer[a] + 100 μL rind crude extract	32520 c[b]
reaction buffer + 100 μL rind crude extract + 100 μL dd H_2O	33900 c
reaction buffer + 100 μL rind crude extract + 100 μL flesh crude extract	17870 b
reaction buffer + 100 μL rind crude extract + 600 μL flesh crude extract	230 a
reaction buffer + 100 μL rind crude extract + 600 μL dd H_2O	32440 c

[a] Described in Materials and Methods. [b] Means followed by different small letter are significantly different at $p \leq 0.05$.

same time when we established maximum mRNA levels (16 h after wounding, not shown). If it is so, a broader experimentation should be addressed to exhaustively analyze the relationship between the de novo synthesized PPO and its role on wounding, for instance, by using 3-methyl-2-bezothiazoline hydrazone (MBTH), (*79*, *80*) which is a good nucleophile that allows the formation of MBTH-adducts with *o*-benzoquinone. MBTH has been demonstrated to increase the sensitivity of the spectrophotometric determination of PPO activity (V_{max} for catechol oxidation in the assay sensitivity to determine MBTH adduct was greater by 12.5-fold than the sensitivity to determine *o*-benzoquinone attributed to the large molar absorptivity of MBTH adduct). Espín et al. (*13*, *59*) confirmed that the method of adding MBTH to reaction mixtures is also effective to determine monophenol oxidase activity of PPO extracted from pears and apples by demonstrating the large molar absorptivity of MBTH adduct as well as short lag periods.

In summary, we have provided a description of the *Ac-ppo* gene of cherimoya fruit and its relationship with PPO activity after wounding. Although numerous manuscripts have described the PPO characteristics in other species, this work is the first study focused to elucidate at the molecular level the role of the PPO gene in the browning process in cherimoya, providing new elements to develop strategies to reduce the PPO impact in fresh cut processing.

ABBREVIATIONS USED

AU, arbitrary units; bps, base pairs; CDS, coding sequence; PPO, polyphenol oxidase; qPCR, real-time quantitative PCR assays; RT-PCR, reverse transcription polymerase chain reaction; HPLC, high performance liquid chromatography; UTR, untranslated region; mRNA, mRNA; U, unit PPO enzyme activity.

LITERATURE CITED

(1) Lee, C. Y.; Whitaker, J. R. Enzymatic browning and its prevention. In *Prevention of Enzymatic Browning in Fruits and Vegetables: A Review of Principles and Practice*; Vamos-Vigyazo, L., Ed.; American Chemical Society: Washington, DC, 1995; pp 49–62.

(2) Nicolas, J. J.; Richard-Forget, F. C.; Goupy, P. M.; Amiot, M. J.; Aubert, S. Y. Enzymatic Browning Reactions in Apple and Apple Products. *Crit. Rev. Food Sci. Nutr.* **1994**, *34*, 109–157.

(3) Steffens, J. C.; Harel, E.; Hunt, M. D. Polyphenol oxidase. In *Genetic Engineering of Plant Secondary Metabolism*; Ellis, B. E., Kuroki, G. W., Stafford, H. A., Eds.; Plenum Press: New York, 1994; *Vol. 28*, pp 275–312.

(4) Mason, H. S. Comparative biochemistry of the phenolase complex. *Adv. Enzymol. Relat. Subj. Biochem.* **1955**, *16*, 105–184.

(5) Mayer, A. M. Polyphenol oxidases in plants and fungi: Going places? A review. *Phytochemistry* **2006**, *67*, 2318–2331.

(6) Fujita, S.; Tono, T. Purification and some properties of polyphenoloxidase in eggplant (*Solanum melongena*). *J. Sci. Food Agric.* **1988**, *46*, 115–123.

(7) Espín, J. C.; García-Ruíz, P. A.; Tudela, J.; García-Cánovas, F. Study of stereospecificity in pear and strawberry polyphenol oxidases. *J. Agric. Food Chem.* **1998**, *46*, 2469–2473.

(8) Castellari, M.; Matricardi, L.; Artelli, G.; Rovere, P.; Amati, A. Effects of high-pressure processing on polyphenoloxidase enzyme activity of grape musts. *Food Chem.* **1997**, *60*, 647–649.

(9) Chevalier, T.; Rigal, D.; Mbéguié-A-Mbéguié, D.; Gauillard, F.; Richard-Forget, F.; Fils-Lycaon, B. R. Molecular cloning and characterization of apricot fruit polyphenol oxidase. *Plant Physiol.* **1999**, *119*, 1261–1270.

(10) Haruta, M.; Murata, M.; Kadokura, H.; Homma, S. Immunological and molecular comparison of polyphenol oxidase in *Rosacea* fruit trees. *Phytochemistry* **1999**, *50*, 1021–1025.

(11) Carbonaro, M.; Mattera, M. Polyphenoloxidase activity and levels in organically grown peach (*Prunus persica* L. cv. Regina bianca) and pear (*Pyrus communis* L. cv. Williams). *Food Chem.* **2001**, *72*, 419–424.

(12) Spagna, G.; Barbagallo, R. N.; Chirasi, M.; Branca, F. Characterization of tomato polyphenol oxidase and its role in browning and lycopene content. *J. Agric. Food Chem.* **2005**, *53*, 2032–2038.

(13) Espín, J. C.; García-Ruíz, P. A.; Tudela, J.; Varón, R.; García-Cánovas, F. Monophenolase and diphenolase reaction mechanisms of apple and pear polyphenol oxidases. *J. Agric. Food Chem.* **1998**, *46*, 2968–2975.

(14) Fenoll, J. G.; Rodríguez-López, J. N.; García-Sevilla, F.; Tudela, J.; García-Ruíz, P. A.; Varón, R.; García-Cánovas, F. Oxidation by mushroom tyrosinase of monophenols generating slightly unstable o-quinones. *Eur. J. Biochem.* **2000**, *19*, 5865–5878.

(15) Marusek, C. M.; Trobaugh, N. M.; Flurkey, W. H.; Inlow, J. K. Comparative analysis of polyphenol oxidase from plant and fungal species. *J. Inorg. Biochem.* **2006**, *100*, 108–123.

(16) van Gelder, C. W.; Flurkey, W. H.; Wichers, H. J. Sequence and structural features of plant and fungal tyrosinases. *Phytochemistry* **1997**, *45*, 1309–1323.

(17) Gerdemann, C.; Eicken, C.; Krebs, B. The crystal structure of catechol oxidase: new insight into the function of type-3 copper proteins. *Acc. Chem. Res.* **2002**, *35*, 183–191.

(18) Sommer, A.; Ne'eman, E.; Steffens, J. C.; Mayer, A. M.; Harel, E. Import, targeting, and processing of a plant polyphenol oxidase. *Plant Physiol* **1994**, *105*, 1301–1311.

(19) Mayer, A. M.; Harel, E. Phenoloxidase and their significance in fruit and vegetables. In *Food Enzymology*; Fox, P. F., Ed.; Elsevier Science Publisher: New York, 1991; pp 373–398.

(20) Ono, E.; Hatayama, M.; Isono, Y.; Sato, T.; Watanabe, R.; Yonekura-Sakakibara, K.; Fukuchi-Mizutani, M.; Tanaka, Y.; Kusumi, T.; Nishino, T.; Nakayama, T. Localization of a flavonoid biosynthetic polyphenol oxidase in vacuoles. *Plant J.* **2006**, *45*, 133–143.

(21) Newman, S. M.; Eannetta, N. T.; Yu, H.; Prince, J. P.; de Vicente, M. C.; Tanskley, S. D.; Steffens, J. C. Organisation of the tomato polyphenol oxidase gene family. *Plant Mol. Biol.* **1993**, *21*, 1035–1051.

(22) Thipyapong, P.; Joel, D. M.; Steffens, J. C. Differential expression and turnover of the tomato polyphenol oxidase gene family during vegetative and reproductive development. *Plant Physiol.* **1997**, *113*, 707–718.

(23) Wang, J.; Constabel, C. P. Biochemical characterization of two differentially expressed polyphenol oxidases from hybrid poplar. *Phytochemistry* **2003**, *64*, 115–121.

(24) Demedina, L. S.; Plata, M. C.; Martínez-Cayuela, M.; Faus, M. J.; Gil, A. Changes in polyphenoloxidase, peroxidase, catalase and acid-phosphatase activities for cherimoya fruit during ripening in controlled temperature and relative-humidity. *Rev. Agroquím. Tecnol. Aliment.* **1986**, *26*, 529–538.

(25) Plata, M. C.; Demedina, L. S.; Martínez-Cayuela, M.; Faus, M. J.; Gil, A. Changes in texture, protein-content and polyphenoloxidase and peroxidase-activities in cherimoya induced by ripening in hypobaric atmospheres or in presence of sulfite. *Rev. Agroquím. Tecnol. Aliment.* **1987**, *27*, 215–224.

(26) Martínez-Cayuela, M.; Demedina, L. S.; Faus, M. J.; Gil, A. Cherimoya (*Annona cherimola* Mill.) polyphenoloxidase - monophenolase and dihydroxyphenolase activities. *J. Food Sci.* **1988**, *53*, 1191–1194.

(27) Martínez-Cayuela, M.; Plata, M. C.; Faus, M. J.; Gil, A. Effect of some phenolic carboxylic-acids on cherimoya (*Annona cherimola*) polyphenoloxidase activity. *J. Sci. Food Agric.* **1988**, *45*, 215–222.

(28) Martínez-Cayuela, M.; Faus, M. J.; Gil, A. Effects of some reductants on the activity of cherimoya polyphenol oxidase. *Phytochemistry* **1988**, *27*, 1589–1592.

(29) Martínez-Cayuela, M.; Rodríguez-Vico, F.; Faus, M. J.; Gil, A. Partial-purification and intracellular-localization of cherimoya (*Annona cherimola Mill*) polyphenoloxidase. *J. Plant Physiol.* **1989**, *133*, 660–663.

(30) Mastrocola, D.; Manzocco, L.; Poiana, M. Prevention of enzymatic browning during freezing, storage and thawing of Cherimoya (*Cherimoya cherimola*, Mill) derivatives. *Ital. J. Food Sci.* **1998**, *10*, 207–215.

(31) Siriphanic, J.; Kader, A. A. Effects of CO_2 on total phenolics, phenyl alanine ammonia lyase and polyphenoloxidase in lettuce tissue. *J. Am. Soc. Hort. Sci.* **1985**, *110*, 249–253.

(32) Bradford, M. M. A rapid and sensitive method for the quantification of microgram quantities of protein utilizing the principle of protein-dye binding. *Anal. Biochem.* **1976**, *72*, 248–254.

(33) Benson, D. A.; Boguski, M. S.; Lipman, D. J.; Ostell, J.; Ouellette, B. F.; Rapp, B. A.; Wheeler, D. L. GenBank. *Nucleic Acids Res.* **1999**, *27*, 12–17.

(34) Hall, T. A. Bioedit: a user friendly biological sequence alignment editor and analysis program for Windows 95/98/NT. *Nucleic Acids Symp. Ser.* **1999**, *41*, 95–98.

(35) Chang, S.; Puryear, J.; Cairney, J. A simple and efficient method for isolating RNA from pine trees. *Plant Mol. Biol. Rep.* **1993**, *11*, 113–116.

(36) Steenkamp, J.; Wild, I.; Lourens, A.; van Helden, P. Improved method for DNA extraction from Vitis vinifera. *Am. J. Enol. Vitic.* **1994**, *45*, 102–106.

(37) Gooding, P. S.; Bird, C.; Robinson, S. P. Molecular cloning and characterisation of banana fruit polyphenol oxidase. *Planta* **2001**, *213*, 748–757.

(38) Demeke, T.; Morris, F. Molecular characterization of wheat polyphenol oxidase (PPO). *Theor. Appl. Genet.* **2002**, *104*, 813–818.

(39) Altschul, S. F.; Madden, T. L.; Schaffer, A. A.; Zhang, J.; Zhang, Z.; Miller, W.; Lipman, D. J. Gapped BLAST and PSI-BLAST: a new generation of protein database search programs. *Nucleic Acids Res.* **1997**, *25*, 3389–3402.

(40) Burge, C. B.; Karlin, S. Finding the genes in genomic DNA. *Curr. Opin. Struct. Biol.* **1998**, *8*, 346–354.
(41) Saitou, N.; Nei, M. The neighbor-joining method: a new method for reconstructing phylogenetic trees. *Mol. Biol. Evol.* **1987**, *4*, 406–425.
(42) Kimura, M. A simple method for estimating evolutionary rates of base substitutions through comparative studies of nucleotide sequences. *J. Mol. Evol.* **1980**, *16*, 111–120.
(43) Bannai, H.; Tamada, Y.; Maruyama, O.; Nakai, K.; Miyano, S. Extensive feature detection of N-terminal protein sorting signals. *Bioinformatics* **2002**, *18*, 298–305.
(44) Bendtsen, J. D.; Nielsen, H.; von Heijne, G.; Brunak, S. Improved prediction of signal peptides: SignalP 3.0. *J. Mol. Biol.* **2004**, *340*, 783–795.
(45) Cuff, J. A.; Barton, G. J. Application of multiple sequence alignment profiles to improve protein secondary structure prediction. *Proteins* **2000**, *40*, 502–511.
(46) Jones, D. T. Protein secondary structure prediction based on position-specific scoring matrices. *J. Mol. Biol.* **1999**, *292*, 195–202.
(47) Bryson, K.; McGuffin, L. J.; Marsden, R. L.; Ward, J. J.; Sodhi, J. S.; Jones, D. T. Protein structure prediction servers at University College London. *Nucleic Acids Res.* **2005**, *33*, W36–38. Web Server issue.
(48) McGuffin, L.; Bryson, K.; Jones, D. T. The PSIPRED protein structure prediction server. *Bioinformatics* **2000**, *16*, 404–405.
(49) Kane, M. D.; Jatkoe, T. A.; Stumpf, C. R.; Lu, J.; Thomas, J. D.; Madore, S. J. Assesment of the sensitivity and specificity of oligonucleotide (50mer) microarrays. *Nucleic Acids Res* **2000**, *28*, 4552–4557.
(50) Cuff, M. E.; Miller, K. I.; van Holde, K. E.; Hendrickson, W. A. Crystal structure of a functional unit from *Octopus hemocyanin*. *J. Mol. Biol.* **1998**, *278*, 855–870.
(51) García-Borrón, J. C.; Solano, F. Molecular anatomy of tyrosinase and its related proteins: beyond the histidine-bound metal catalytic center. *Piament Cell Res.* **2002**, *15*, 162–173.
(52) Sun, D. J.; He, Z. H.; Xia, X. C.; Zhang, L. P.; Morris, C. F.; Appels, R.; Ma, W. J.; Wang, H. A novel STS marker for polyphenol oxidase activity in bread wheat. *Mol. Breed.* **2005**, *16*, 209–218.
(53) Richter, H.; Lieberei, R.; von Schwartzenberg, K. Identification and characterization of a Bryophyte polyphenol oxidase encoding gene from *Physcomitrella patens*. *Plant Biol. (Stuttgart)* **2005**, *7*, 283–291.
(54) Haruta, M.; Pedersen, J. A.; Constable, C. P. Polyphenol oxidase and herbivore defense in trembling aspen (*Populus tremuloides*): cDNA cloning, expression, and potential substrates. *Physiol. Plant* **2001**, *112*, 552–558.
(55) Li, L.; Steffens, J. C. Overexpression of polyphenol oxidase in transgenic tomato plants results in enhanced bacterial disease resistance. *Planta* **2002**, *215*, 239–247.
(56) Gardiazabal, F.; Rosenberg, G. *El Cultivo del Chirimoyo*; Ediciones Universitarias de Valparaíso: Valparaíso, Chile,1993; pp 1–145.
(57) Cheng, T.; Huang, P.; Pan, J.; Lin, K.; Mao, S. Gel electrophoresis of polyphenol oxidase with instant identification in situ blotting. *J. Chromatogr. B* **2007**, *849*, 331–336.
(58) Espín, J. C.; Varón, R.; Tudela, J.; García-Cánovas, F. Kinetic study of the oxidation of 4-hydroxyanisole catalyzed by tyrosinase. *Biochem. Mol. Biol. Int.* **1997**, *41*, 1265–1276.
(59) Espín, J. C.; Tudela, J.; García-Cánovas, F. 4-hydroxyanisole: The most suitable monophenolic substrate for determining spectrophotometrically the monophenolase activity of polyphenol oxidase from fruits and vegetables. *Anal. Biochem.* **1998**, *259*, 118–126.
(60) Sullivan, M. L.; Hatfield, R. D.; Thoma, S. L.; Samac, D. A. Cloning and characterization of red clover polyphenol oxidase cDNAs and expression of active protein in Escherichia coli and transgenic alfalfa. *Plant Physiol.* **2004**, *136*, 3234–3244.
(61) Martínez-Cayuela, M.; Plata, M. C.; Faus, M. J.; Gil, A. Effect of some phenolic carboxylic acids on cherimoya (*Annona cherimolia*) polyphenoloxidase activity. *J. Sci. Food Agric.* **1988**, *45*, 215–222.
(62) Cánovas, F. G.; Tudela, J.; Madrid, C. M.; Varón, R.; Carmona, F. G.; Lozano, J. A. Kinetic-study on the suicide inactivation of tyrosinase induced by catechol. *Biochim. Biophys. Acta* **1987**, *912*, 417–423.
(63) Tudela, J.; Cánovas, F. G.; Varón, R.; Jimenez, M.; Garciacarmona, F.; Lozano, J. A. Kinetic-study in the transient phase of the suicide inactivation of frog epidermis tyrosinase. *Biophys. Chem.* **1988**, *30*, 303–310.
(64) Rathjen, A. H.; Robinson, S. P. Aberrant processing of polyphenol oxidase in variegated grapevine mutant. *Plant Physiol.* **1992**, *99*, 1619–1625.
(65) Espín, J. C.; van Leeuwen, J.; Wichers, H. J. Kinetic study of the activation process of a latent mushroom (Agaricus bisporus) tyrosinase by serine proteases. *J. Agric. Food Chem.* **1999**, *47*, 3509–3517.
(66) Espín, J. C.; Wichers, H. J. Kinetics of activation of latent mushroom (Agaricus bisporus) tyrosinase by benzyl alcohol. *J. Agric. Food Chem.* **1999**, *47*, 3503–3508.
(67) Anosike, E. O.; Ayaebene, A. O. Purification and some properties of polyphenol oxidase from the yam tubers, *Dioscorea bulbifera*. *Phytochemistry* **1981**, *202*, 625–2628.
(68) Arslan, O.; Temur, A.; Tozlu, I. Polyphenol oxidase from Allium sp. *J. Agric. Food Chem.* **1997**, *452*, 861–2863.
(69) Owusu-Ansah, Y. J. Polyphenoloxidase in wild rice (*Zizania palustris*). *J. Agric. Food Chem.* **1989**, *37*, 901–904.
(70) Oktay, M.; Lufrevioglu, I.; Kocacaliskan, I.; Sakiroqlu, H. Polyphenoloxidase from Amasya apple. *J. Food Sci.* **1995**, *60*, 494–496.
(71) González, E. M.; Ancos, B. D.; Cano, M. P. Partial characterization of peroxidase and polyphenol oxidase activities in blackberry fruits. *J. Agric. Food Chem.* **2000**, *48*, 5459–5464.
(72) Paul, B.; Gowda, L. R. Purification and characterization of a polyphenol oxidase from the seeds of field bean (*Dolichos lablab*). *J. Agric. Food Chem.* **2000**, *48*, 3839–3846.
(73) Kavrayan, D.; Aydemir, T. Partial purification and characterization of polyphenoloxidase from peppermint (*Mentha piperita*). *Food Chem.* **2001**, *74*, 147–54.
(74) Serradell, M. A.; Rozenfeld, P. A; Martínez, G. A.; Civello, P. M.; Chaves, A. R.; Anon, M. C. Polyphenoloxidase activity from strawberry fruit (*Fragaria x ananassa*, Duch., cv. Selva): characterization and partial purification. *J. Sci. Food Agric.* **2000**, *80*, 1421–1427.
(75) Fraignier, M. P.; Marques, L.; Fleuriet, A.; Macheix, J. J. Biochemical and immunochemical characteristics of polyphenol oxidases from different fruit of Prunus. *J. Agric. Food Chem.* **1995**, *43*, 2375–2380.
(76) Aydemir, T. Partial purification and characterization of polyphenol oxidase from artichoke (*Cynara scolymus L.*) heads. *Food Chem.* **2004**, *87*, 59–67.
(77) Nagai, T.; Suzuki, N. Polyphenol oxidase from bean sprouts (*Glycine max L.*). *J. Food Sci.* **2003**, *68*, 16–20.
(78) Martínez, M. V.; Whitaker, J. R. The biochemistry and control of enzymatic browning. *Trends Food Sci. Technol.* **1995**, *6*, 195–200.
(79) Rodríguez-López, J. N.; Escribano, J.; García-Cánovas, F. A continuous spectrophotometric method for the determination of monophenolase activity of tyrosinase using 3-methyl-2-benzothiazolinone hydrazone. *Anal. Biochem.* **1994**, *216*, 205–212.
(80) Espín, J. C.; Varón, R.; Fenoll, L.; Gilabert, A.; García-Ruíz, P.; Tudela, J.; García-Cánovas, F. Kinetic characterization of the substrate specificity and mechanism of mushroom tyrosinase. *Eur. J. Biochem.* **2000**, *267*, 1270–1279.

Received for review February 28, 2007. Revised manuscript received June 27, 2007. Accepted July 13, 2007. This work was supported by FONDECYT 1040011.

JF070586+